Exergy analysis of two-phase steam-water injector

Marian Trela, Roman Kwidzinski, Dariusz Butrymowicz

▶ **To cite this version:**

Marian Trela, Roman Kwidzinski, Dariusz Butrymowicz. Exergy analysis of two-phase steam-water injector. Applied Thermal Engineering, 2009, 30 (4), pp.340. 10.1016/j.applthermaleng.2009.09.011 . hal-00528084

HAL Id: hal-00528084
https://hal.science/hal-00528084v1

Submitted on 21 Oct 2010

HAL is a multi-disciplinary open access archive for the deposit and dissemination of scientific research documents, whether they are published or not. The documents may come from teaching and research institutions in France or abroad, or from public or private research centers.

L'archive ouverte pluridisciplinaire **HAL**, est destinée au dépôt et à la diffusion de documents scientifiques de niveau recherche, publiés ou non, émanant des établissements d'enseignement et de recherche français ou étrangers, des laboratoires publics ou privés.

Accepted Manuscript

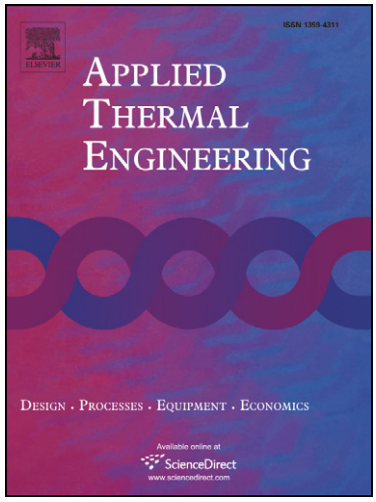

Exergy analysis of two-phase steam-water injector

Marian Trela, Roman Kwidzinski, Dariusz Butrymowicz, Dariusz Butrymowicz

PII: S1359-4311(09)00283-X
DOI: 10.1016/j.applthermaleng.2009.09.011
Reference: ATE 2890

To appear in: *Applied Thermal Engineering*

Received Date: 25 June 2008
Accepted Date: 18 September 2009

Please cite this article as: M. Trela, R. Kwidzinski, D. Butrymowicz, D. Butrymowicz, Exergy analysis of two-phase steam-water injector, *Applied Thermal Engineering* (2009), doi: 10.1016/j.applthermaleng.2009.09.011

This is a PDF file of an unedited manuscript that has been accepted for publication. As a service to our customers we are providing this early version of the manuscript. The manuscript will undergo copyediting, typesetting, and review of the resulting proof before it is published in its final form. Please note that during the production process errors may be discovered which could affect the content, and all legal disclaimers that apply to the journal pertain.

ACCEPTED MANUSCRIPT

reference: **ATE 2890**

full title: Exergy analysis of two-phase steam-water injector

author 1: Marian Trela
affiliation: University of Warmia and Mazury, Faculty of Technical Sciences, Oczapowskiego 11, 10-957 Olsztyn, Poland

author 2: Roman Kwidzinski
affiliation: The Szewalski Institute of Fluid-Flow Machinery, Polish Academy of Sciences, Fiszera 14, 80-231 Gdansk, Poland

author 3: Dariusz Butrymowicz
affiliation: The Szewalski Institute of Fluid-Flow Machinery, Polish Academy of Sciences, Fiszera 14, 80-231 Gdansk, Poland

author 4: Jaroslaw Karwacki
affiliation: The Szewalski Institute of Fluid-Flow Machinery, Polish Academy of Sciences, Fiszera 14, 80-231 Gdansk, Poland

contact information for the corresponding author:

postal address: Roman Kwidzinski
The Szewalski Institute of Fluid-Flow Machinery, PASc
ul. Fiszera 14
80-231 Gdansk
Poland

e-mail: rk@imp.gda.pl

phone: +48 58 6995163

fax: +48 58 3416144

Abstract:

Exergy analysis is used as a tool for the evaluation of exergy losses in a two-phase steam-water injector in an effort to improve its overall performance in respect to exit pressure. The aim of this paper is to study irreversible losses in the component parts of the injector, including the steam nozzle, water nozzle and diffuser as well as the two-phase region comprising the mixing chamber and the condensation shock wave. Calculations based on experimental data revealed the regions with the greatest irreversibilities, namely in the two-phase region and in the steam nozzle. Particular attention was paid to the steam nozzle, for which a procedure was developed to determine the overall velocity coefficient, including all irreversibilities in the steam nozzle during steam expansion. The study indicated the most important factors influencing the injector's performance. Finally, the exergy efficiency was calculated for the two investigated steam injectors.

Keywords:

exergy, steam-water injector, jet pump

ACCEPTED MANUSCRIPT

ACCEPTED MANUSCRIPT

Nomenclature

A	cross-section surface area, m^2
b	specific thermal exergy, J/kg
$\dot{B}$	exergy transfer rate, W
c_v	velocity coefficient, $c_v = w_1/w_{1s}$, dimensionless
G	water volumetric flow rate, m^3/h
h	specific enthalpy, J/kg
I	exergy destruction (due to irreversibility), W
$\dot{m}$	mass flow rate, kg/s
p	pressure, Pa
$\dot{Q}$	heat transfer rate, W
s	specific entropy, J/kgK
$\dot{S}_g$	entropy generation rate, W/K
T	temperature, K or °C
T_r	reference temperature, $T_r = 273.16$ K
U	entrainment ratio, $U = \dot{m}_{L0}/\dot{m}_{V0}$
w	velocity, m/s
x	steam quality (dryness fraction), dimensionless
z	axial coordinate, distance from mixing chamber inlet, m

Greek symbols

η	efficiency, dimensionless
η_{SN}	steam nozzle efficiency, $\eta_{SN} = (w_{V1}/w_{V1s})^2 = c_v^2$
ρ	density, kg/m^3
ζ	hydraulic resistance coefficient, dimensionless
ψ	flow exergy, J/kg

Subscripts

a	average
B	exergy
CV	control volume
d	dead state
DF	diffuser
dry	dry steam flow
f	frictional
irr	irreversible
L	liquid (water)
MC	mixing chamber
V	vapour (steam)
s	isentropic value
t	total
SI	steam-water injector
SN	steam nozzle
SW	shock wave
WN	water nozzle
0	at steam injector inlet (for steam and water)
1	at mixing chamber inlet
2	at mixing chamber throat
3	at high-pressure side of condensation shock wave
4	at steam injector outlet

ACCEPTED MANUSCRIPT

ACCEPTED MANUSCRIPT

1. Introduction

The two-phase vapour-liquid injector (or ejector) is a simple, compact device in which the thermal energy of vapour is used to heat or pump liquid. Such an injector can work as a passive (i.e. not requiring an electric power supply) jet pump or as an efficient direct-contact heater. Due to its advantages, the injector is applied in many areas of industry, e.g. in thermal engineering, refrigeration and air conditioning, desalination as well as in the petrochemical and chemical industries [1]. In chemical engineering two-phase injectors are used as mixers, reactors or absorbers [2,3].

Various vapours and liquids are used in two-phase injectors. If water is used, with its vapour (i.e. steam) as a primary stream and water in liquid state as a secondary stream, the device is called a steam-water injector (SI – when used to raise water pressure) or a steam-water ejector (when primarily used to suck water from a reservoir) . The steam-water injector consists of four main parts: steam nozzle (SN), water nozzle (WN), mixing chamber (MC) and diffuser (DF). Such an injector with a central steam nozzle arrangement is shown in Fig. 1. Superheated steam is expanded and accelerated to a supersonic velocity in the converging-diverging nozzle (Laval type). This creates a low static pressure at the MC inlet, which causes water to be drawn in through the annular slot (gap) surrounding the steam nozzle exit. In the mixing chamber, the steam transfers its momentum and energy to the water. The resulting two-phase flow is compressed in the shock wave forming in the diffuser downstream of the throat. Inside the shock wave region the vapour phase completely condenses. Thus only liquid water leaves the steam-water injector.

The flow of steam and water in the mixing chamber is very complex. Due to mass, momentum and energy transfer between the phases, different flow patterns or flow regimes appear in the MC [4].

Many papers have been published in an effort to improve the understanding of injector/ejector processes and their performance. However, our knowledge of the physical mechanisms occurring in this device is still limited. Two different general methodologies have been used to tackle this problem. The first one proposes models, e.g. [5,6,7], describing the global thermal and flow characteristics of the injector and uses the experimental results to close the model equations [5]. A more detailed description of the injector flow has been obtained from models based on conservation equations formulated in the cases of 1D [6] or 2D [7]. The second approach is based on exergy analysis, which can be applied to particular parts of the injectors in order to find the exergy losses occurring there and this way evaluate the injector's performance. Arbel et al. [8] proposed entropy production methodology for one-phase gas-gas ejectors to find performance losses during internal processes on the basis of Gouya-Stodola's well-known theorem, where the entropy generation is proportional to exergy losses. Pridasawas and Lundqvist [9] used exergy analysis as a tool to analyse the performance of a gas-gas ejector refrigeration cycle driven by solar energy. They found that the most significant exergy losses in the system occurred in the solar collector and in the ejector. Yari and Sirousazar [10] analysed the performance of a new configuration ejector–vapour compression refrigeration cycle using the exergy method.

Trela and Kwidzinski [11] and Trela et al. [12] carried out both an experimental and theoretical investigations on two-phase steam-water injectors. They found that the most

ACCEPTED MANUSCRIPT

significant exergy losses were in the two-phase region (TP) (including mixing chamber and shock wave) and in the steam nozzle. Two different methods were used for the TP region. In the first (direct) method, an entropy balance equation for a control volume comprising the two-phase region was applied [13]. In the second method, the exergy losses in the two-phase region were evaluated indirectly as the difference between the steam and water exergy sum at the steam injector inlet and the sum comprising exit water exergy plus the exergy losses in the steam nozzle, water nozzle and diffuser. The authors of [11,12] argued that the indirect method was more precise because it took into account non-equilibrium aspects, which was not possible in the direct method.

The aim of this paper is to present the methodology of exergy losses evaluation in component parts of the steam injector with special attention focused on the steam nozzle. The flow of steam in the Laval nozzle may be very complicated if the steam expansion line enters a wet steam region (i.e. below the saturation line). To determine the exergy losses in the nozzle in such cases a special procedure has been developed. This procedure is presented in the paper with example calculations based on the experimental results obtained for two versions of the steam injector.

2. Experimental set-up

Experimental investigations of the steam-water injector were conducted on two laboratory scale injectors (Fig.2) designed and built at the Szewalski Institute of Fluid-Flow Machinery (IFFM) in Gdańsk. In both these injectors the water flowed in the form of a thin annular film on the mixing chamber wall with the steam in the mixing chamber core. The measured and recorded parameters of the inlet steam and water included: temperature, pressure and flow rate. Measured also were the distributions of average pressure, temperature and void fraction along the mixing chamber and diffuser. Flow rates were measured with an accuracy of 1.25%, pressure – 0.1% and temperature – 0.2 K. The design of the injectors to some extent allowed for variations of inter-phase exchange conditions in the mixing chamber by adjusting the size of the annular water nozzle gap [4, 14].

Two different steam injectors were used. In the first one (the so-called long version) the mixing chamber length was 220 mm and the average mixing chamber pressure was $p_{MC} = 7$ kPa, while the mixing chamber of second, short version was 100 mm long and its average mixing chamber pressure was $p_{MC} = 19$ kPa. Figure 3 shows the short version steam-water injector with some details of pressure transducers and thermocouple arrangement.

During experimental investigations the inlet steam parameters and the inlet water temperature were kept constant. The exit pressure was adjusted to its maximum value with the condensation wave located at the MC throat. Any further attempt to increase the back-pressure and push the condensation wave deeper into MC throat destabilized the flow in the SI and caused the apparatus to stall.

3. Experimental results

The profiles of pressure p and temperature T obtained during the research are typical for the two-phase steam-water injector. Example results for both SI versions are shown in Fig. 4 (SI with long MC) and in Fig. 5 (SI with short MC). These show that the MC pressure profiles

ACCEPTED MANUSCRIPT

are flat, while the temperature rises in near-linear way. A rapid pressure rise is observed only in the shock wave region, followed by a further, moderate increase of pressure along the diffuser. The measurements were taken with the inlet parameters having the following values: steam flow 128 ± 5 kg/h, absolute steam pressure 3.8 ± 0.1 bar, steam superheating 13–29 ºC, water flow 1.5–6.0 m^3/h, inlet water temperature 13.8–18.6 ºC, water nozzle gap 1.0 mm.

Two facts are worth noting. Firstly, the change of pressure in the SI diffuser does not propagate upstream of the shock wave region. This means that the two-phase flow in the mixing chamber is supercritical. Secondly, the exit pressure can exceed the inlet vapour pressure when there is a sufficiently high water-to-vapour mass flow ratio, i.e. entrainment ratio U (see Fig. 5). The highest exit-water-to-inlet-steam-pressure ratio achieved for the "short" SI was 1.24 while for "long" SI this parameter reached only 0.86 in similar inlet flow conditions [15,16]. When the values of water flow rate G are low, the exit pressure diminishes but the water temperature rises higher. However, in this case the shock wave shifts downstream and the two-phase flow extends further into diffuser.

4. Evaluation of exergy losses

From the thermodynamic point of view, the steam-water injector is an example of an open system (control volume). An exergy balance in the control volume can be expressed in a rate form as [13]

$$\dot{B}_{heat} - \dot{B}_{work} + \dot{B}_0 - \dot{B}_4 - I_{SI} = \Delta\dot{B}_{CV}\,, \tag{1}$$

taking into account the rates of exergy transfer by heat, work and mass. During normal injector operation the flow is steady ($\Delta\dot{B}_{CV} = 0$), the heat transfer to the surroundings is negligibly small ($\dot{B}_{heat} \approx 0$) and the work is nil ($\dot{B}_{work} = 0$) so Eq. (1) is reduced to

$$\dot{B}_0 - I_{SI} = \dot{B}_4\,, \tag{2}$$

where I_{SI} stands for all irreversible losses in the steam injector and symbols $\dot{B}_0, \dot{B}_4$ denote the exergy transfer rate at the injector inlet and outlet, respectively.

Irreversible losses are generated in four different regions of the flow domain in the injector, namely in the steam nozzle (SN), water nozzle (WN), two-phase flow region (TP) and diffuser (DF). Thus, the total losses I_{SI} may be written as a sum

$$I_{SI} = I_{SN} + I_{WN} + I_{TP} + I_{DF}\,. \tag{3}$$

If the performance of the two-phase (steam-water) injector is assessed, it is important to know exergy destruction in all of the above-mentioned regions. Except for the mixing chamber and shock wave regions, the exergy losses can be evaluated using the general thermodynamic approach presented in textbooks, e.g. [13,17]. The results obtained by Trela and Kwidzinski [11] show that exergy destruction in the single-phase flow regions of the injector can be evaluated according to the following formulas:

<u>for steam nozzle</u>

ACCEPTED MANUSCRIPT

$$I_{SN} = \dot{m}_{V0}\,\Delta h_{irr\,SN} = \dot{m}_{V0}\left(h_{V0} + \frac{w_{V0}^2}{2} - h_{V1s} \right)(1 - c_v^2) \tag{4}$$

where, using the nomenclature shown in Fig.6, $\Delta h_{irr\,SN}$ is given as

$$\Delta h_{irr\,SN} = (h_{V0} + \frac{w_{V0}^2}{2} - h_{V1s})(1 - c_v^2) = (h_{V0t} - h_{V1s})(1 - c_v^2) \tag{4a}$$

for water nozzle

$$I_{WN} = T_r \dot{S}_{g\,WN} = T_r \zeta \frac{\dot{m}_{L0}^3}{2T_{L\,WN}\rho_L^2 A_{L1}^2} \tag{5}$$

for diffuser

$$I_{DF} = T_r\, \dot{S}_{g\,DF} = T_r \zeta \frac{(\dot{m}_{V0} + \dot{m}_{L0})^3}{2T_{L\,DF}\rho_L^2 A_{L3}^2} \tag{6}$$

It is far more more difficult to evaluate exergy loss for the two-phase flow (TP) region, comprising the mixing chamber (MC) and shock wave region (SW), where mass, momentum and energy transfer between vapour and liquid plays a dominant role. The difficulties arise from the very complex nature of the phenomena occurring in this flow region, where three irreversible processes – friction, flow pattern transitions and steam-water heat transfer, contribute to exergy destruction. Moreover, the flow in the mixing chamber is not in equilibrium since the temperatures of water and steam differ significantly. Therefore, due to a lack of sufficiently detailed information on the flow structure and the thermodynamic parameters of the steam and water, this flow region is treated globally and the exergy destruction I_{TP} is calculated by the above mentioned indirect method. Thus, taking the advantage of Eqs (2)–(6), the value of I_{TP} is calculated using the balance equation

$$I_{TP} = \dot{B}_0 - \dot{B}_4 - I_{SN} - I_{WN} - I_{DF}\,. \tag{7}$$

The inlet exergy $\dot{B}_0$ is a sum of contributions from the inlet steam and water,

$$\dot{B}_0 = \dot{B}_{V0} + \dot{B}_{L0}, \tag{8}$$

while the outlet exergy $\dot{B}_4$ is determined from flow properties at the steam injector exit (state 4). The respective exergies are calculated as [13,11]

$$\dot{B}_{V0} = \dot{m}_{V0}\left(h_{V0} - T_r s_{V0} + \frac{w_{V0}^2}{2} \right) \tag{9}$$

$$\dot{B}_{L0} = \dot{m}_{L0}\left(h_{L0} - T_r s_{L0} + \frac{w_{L0}^2}{2} \right) \tag{10}$$

$$\dot{B}_4 = (\dot{m}_{V0} + \dot{m}_{L0})\left(h_{L4} - T_r s_{L4} + \frac{w_{L4}^2}{2} \right) \tag{11}$$

In the above equations the reference temperature T_r should correspond to a state for which entropy is set to zero (usually the triple state, in which case T_r = 273.16 K).

ACCEPTED MANUSCRIPT

Evaluation of the exergy losses I_{SN} in the steam nozzle, I_{WN} in the water nozzle and I_{DF} in the diffuser requires knowledge of the velocity coefficient c_v for the steam nozzle and flow resistance coefficients ζ for the water nozzle and diffuser. The evaluation of the two coefficients ζ is quite easy since they depend on the geometry of the nozzle and diffuser, respectively, as well as on the flow conditions expressed by Reynolds number [18]. The approximate values of ζ are in the range 0.1–0.2.

Evaluation of coefficient c_v

Determination of coefficient c_v is not an easy task when superheated steam expands in a Laval nozzle to a pressure below the Wilson line (when spontaneous steam condensation causes additional exergy losses). It should be pointed out that under working conditions the mixing chamber pressure may be different from the nominal pressure at the steam nozzle exit, which causes a shock wave formation and also generates additional exergy losses. A schematic representation of the expansion line in the Laval nozzle is shown in the *h-s* diagram, Fig. 6.

Here four major sources of exergy losses may be distinguished: friction, spontaneous condensation, the flow of the steam-droplet mixture and the shock wave at the nozzle exit (when the exit pressure does not match the inlet MC pressure). The first three phenomena may be taken into account using the well-known Baumann rule [19],

$$\eta_{SN} = \eta_{SN\,dry}\; x_a \tag{12}$$

in which the steam nozzle efficiency η_{SN} is equal to the product of nozzle efficiency in dry stream conditions $\eta_{SN\,dry}$ and the average steam quality x_a during steam expansion. It follows from Eq. (12) that for constant inlet steam conditions, the average steam quality is proportional to the exit steam quality x_1 only, thus efficiency η_{SN} can be presented as

$$\eta_{SN} \approx (c_v)^2_{dry}\; x_1 \tag{13}$$

A special numerical procedure was developed to calculate the overall velocity coefficient c_v in this complex case using experimental data to determine the conditions at the steam nozzle inlet and exit. With the measured values of the inlet steam pressure p_{V0} and temperature T_{V0}, as well as of the exit pressure p_{V1} in the mixing chamber (at a location less than 1 mm from the steam nozzle outlet), the iterative method was used to find such a value of c_v where the calculated steam mass flow rate $\dot{m}_{V1}$ was equal to the measured value $\dot{m}_{V0}$.

In each iteration the ideal-flow exit enthalpy $h_{V1s}(p_{V1},s_{V0})$ was calculated first (Fig. 6), assuming isentropic expansion in the steam nozzle, i.e. at the condition $s_{V1s} = s_{V0}$. Next, using an approximate value of the velocity coefficient c_v, enthalpy loss $\Delta h_{irr\,SN}$ was evaluated from Eq. (4a). Adding $\Delta h_{irr\,SN}$ and h_{V1s}, a value of exit enthalpy h_{V1} in irreversible flow was found,

$$h_{V1} = \Delta h_{irr\,SN} + h_{V1s}\,. \tag{14}$$

This enthalpy was used to determine vapour density at the steam nozzle exit, $\rho_{V1}(p_{V1},h_{V1})$. Furthermore, steam nozzle exit velocity w_{V1} was evaluated [11] from

$$w_{V1} = c_v \sqrt{2\left(h_{V0} - h_{V1s}\right)}\,. \tag{15}$$

ACCEPTED MANUSCRIPT

Finally, the steam mass flow rate at the nozzle exit (of cross-section area $A_{1\,SN}$) was calculated as

$$\dot{m}_{V1} = A_{1\,SN}\rho_{V1}w_{V1} \tag{16}$$

and compared with the measured value $\dot{m}_{V0}$.

The Newton numerical method was applied to eliminate the initial discrepancy between the values of $\dot{m}_{V0}$ and $\dot{m}_{V1}$ and to determine the correct value of c_v. When the pressure tap was located downstream of the nozzle exit plane at a distance exceeding 1 mm, a parabolic extrapolation was used to get the correct value of the nozzle exit pressure p_{V1}.

Results of the c_v calculations for the "short" and "long" version steam injectors are shown in Fig. 7. The values obtained generally are lower than usually assumed for Laval-type nozzles (0.94–0.99 [13]), suggesting that additional irreversible losses are encountered due to spontaneous condensation and shock wave formation in the supersonic steam flow near the nozzle exit. Indeed, calculated steam quality at the nozzle exit indicated the presence of wet steam. Moreover, the measured pressure p_{V1} was higher than the design (nominal) exit value for the steam nozzles of both steam injectors.

The results of the calculation of the exergy losses in injector parts are shown in Fig. 8. The calculations were based on data gathered in the experiments described above, with a constant steam flow rate at the injector inlet and with selected inlet-water flow rates to obtain entrainment ratio U in the range 12–47. The measured flow rates, temperature and pressure were used to calculate exergy at the injector's inlet and outlet as well as the exergy losses in its component parts according to Eqs. (4)–(7). Total steam injector exergy losses calculated according to Eq. 3 are shown in Fig. 9.

Finally, the exergy efficiency η_B of the steam-water injector was calculated as

$$\eta_B = \frac{\dot{B}_4}{\dot{B}_0} \tag{17}$$

The results shown in Fig. 10 indicate that the efficiency is the highest for low values of entrainment ratio U, reaching 36% when $U = 16$ in "long" SI and falling to 28% when $U = 47$. For the "short" SI, the efficiency varied from 44% to 36% when the U ratio range was 12–38.

5. Concluding remarks

The above analysis was based on the methodology of entropy production applied to the two-phase steam-water injector. Since the entropy production is equivalent to exergy destruction, a procedure based on the experimental data was developed to evaluate exergy losses in the injector parts. This procedure showed that the highest irreversibility sources are in the two-phase region (mixing chamber and condensation shock) and in steam nozzle.

Special attention was paid to the steam nozzle flow, for which a method was devised to calculate the overall velocity coefficient, including all irreversibility sources during the expansion of motive steam in the Laval nozzle. Since initially superheated steam expands in the Laval nozzle below the saturation and Wilson lines, four irreversibility sources were identified: friction, spontaneous condensation, steam-water droplet mixture flow and the shock wave at the steam nozzle exit.

ACCEPTED MANUSCRIPT

Using the experimental data, the overall velocity coefficient was calculated for the two test steam-water injectors working at the same initial steam parameters. It turned out that the coefficient values for the two injectors differ significantly. For the short steam nozzle, in which the expansion line terminates at higher pressure and therefore with a higher exit steam quality, the velocity coefficient is greater. This fact evidently shows the importance of steam quality on injector performance. By selecting proper steam parameters at the steam nozzle exit this source of irreversibility may be significantly reduced and injector performance, in respect of the exit pressure, increased.

Calculations of the velocity coefficient and injector exergy efficiency revealed their strong dependence on entrainment ratio U, which results from irreversibility loss changes in the injector elements. Contrary to the common opinion that steam-water injectors have very poor efficiency, this analysis indicates that the exergy efficiency of the injector can be quite high, from 27% to 45%.

References

[1] H. El-Dessouky, H. Ettouney, I. Alatiqi, G. Al-Nuwaibit, Evaluation of steam jet ejectors, Chemical Engineering and Processing 41 (2002), 551–561.

[2] A. Sözen, G. Arcaklioğlu, Exergy analysis of an ejector-absorption heat transformer using artificial neural network approach, Applied Thermal Engineering 27 (2007), 481-491.

[3] C. Dang, S. Nakamura, Y. Lee, J. Wang, A mixing type absorber in absorption refrigeration system, Proc. of The 2nd Asian Conference on Refrigeration and Air-Conditioning (ACRA), Beijing, China, May 12-13, 2004, 441.

[4] M. Trela, R. Kwidziński, D. Butrymowicz, A. Jaworek, P. Dumaz, Studies of physical phenomena of two-phase flow in steam-water injector, Proc. of The 11th International Topical Meeting on Nuclear Reactor Thermal-Hydraulics (NURETH-11), Avignon, France, October 2-6, 2005, CD-ROM, Paper No. 090.

[5] N. Deberne, J.F. Leone, A. Duque, A. Lallemand, A model for calculation of steam injector performance, International Journal of Multiphase Flow 25 (1999), 841-855.

[6] N. Beithou, H.S. Aybar, High-Pressure Steam-Driven Jet Pump – Part I: Mathematical Modeling, Journal of Engineering for Gas Turbines and Power (Transactions of the ASME) 123 (2001), 693-700.

[7] T. Narabayashi, M. Mori, M. Nakamaru, S. Ohmori, Study on two-phase flow dynamics in steam injectors. II. High pressure tests using scale-models, Nuclear Engineering and Design 200 (2000), 261-271.

[8] A. Arbel, A. Shklyar, D. Hershgal, M. Barak, M. Sokolov, Ejector irreversibility characteristics, Journal of Fluids Engineering 125 (2003), 121-129.

[9] W. Pridasawas, P. Lundqvist, An exergy analysis of a solar-driven ejector refrigeration system, Solar Energy 76 (2004), 369–379.

[10] M. Yari, M. Sirousazar, Performance analysis of the ejector-vapour refrigeration cycle, Proc. IMechE Vol. 221, Part A: J. Power and Energy, 2007, 1089-1098.

[11] M. Trela, R. Kwidziński, Exergy analysis of steam-water performance**,** Archives of Thermodynamics 29 (1) (2008), 41-58.

ACCEPTED MANUSCRIPT

[12] M. Trela, R. Kwidziński, D. Butrymowicz, Exergy analysis of losses in a two-phase steam-water injector, Chemical and Process Engineering, 29 (2008), 455-466.

[13] Y.A. Cengel, M.A. Boles, Thermodynamics – An Engineering Approach, McGraw Hill Book Company, 2002.

[14] M. Trela, D. Butrymowicz, P. Dumaz, Experimental investigation of heat transfer in steam-water injector, Proc. of The 5th Int. Conference Multiphase Flow (ICMF-2004) Yokohama, May 2004, Paper 544.

[15] M. Trela, R. Kwidziński, M. Buła, Maximum discharge pressure of supercritical two-phase steam injector, Archives of Thermodynamics 25 (1) (2004), 41-52

[16] R. Kwidziński, M. Trela, Investigation of steam-water injector with various mixing chamber throat shapes (in Polish), Proc. of XIII Sympozjum Wymiany Ciepła i Masy 2007, Koszalin – Darłówko, Poland, Vol. 2 (2007), 641-648.

[17] J.F. Douglas, J.M. Gasiorek, J.A. Swaffield, Fluid Mechanics (4th Edition), Pearson Prentice Hall, London, 2001.

[18] I.E. Idelchik, Handbook of Hydraulic Resistance (3rd Edition), Begell House, New York, 1996.

[19] M. J. Moore, C. H. Sieverding, Two-phase steam flow in turbines and separators: Theory, Instrumentation, Engineering, Hemisphere Publishing Corporation, Washington, London, 1976.

ACCEPTED MANUSCRIPT

ACCEPTED MANUSCRIPT

Figure 1

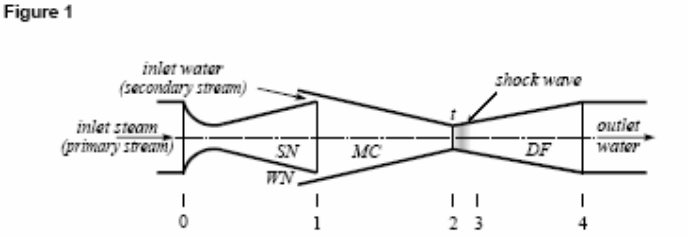

ACCEPTED MANUSCRIPT

ACCEPTED MANUSCRIPT

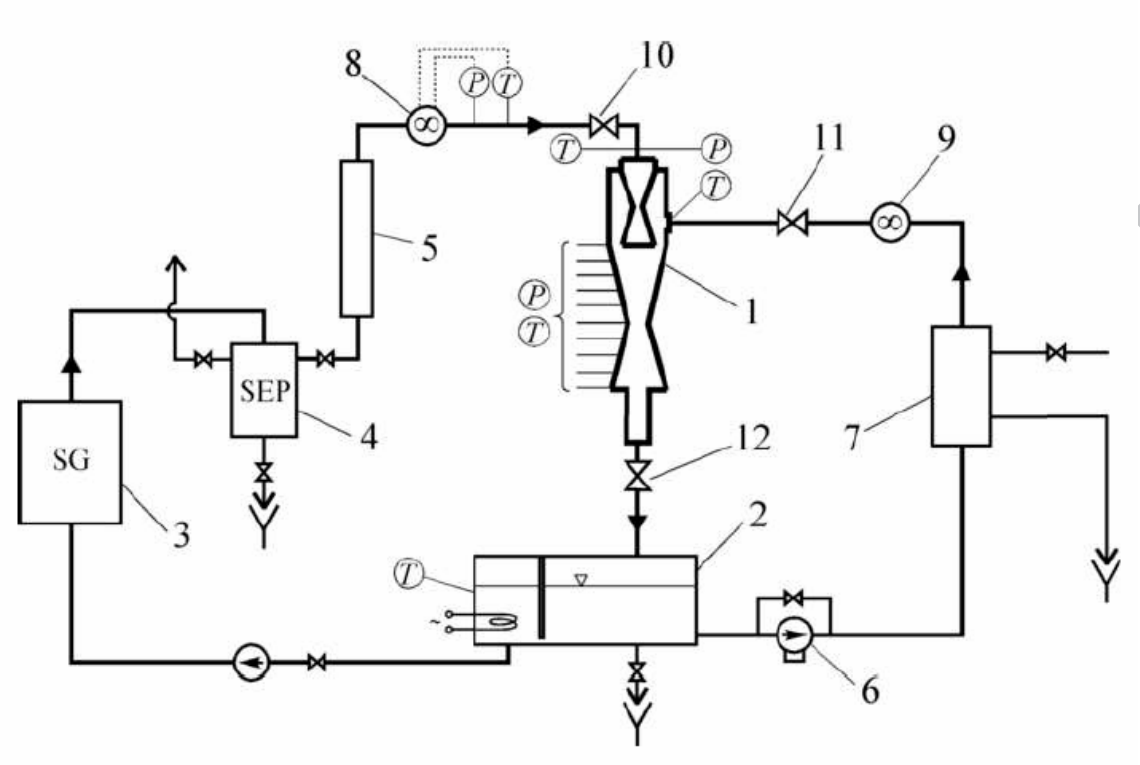

ACCEPTED MANUSCRIPT

ACCEPTED MANUSCRIPT

Figure 3

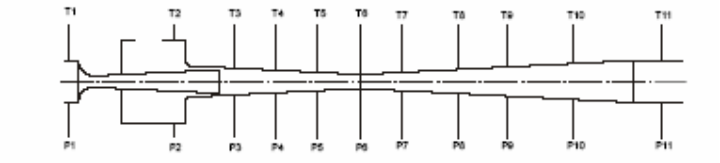

ACCEPTED MANUSCRIPT

ACCEPTED MANUSCRIPT

Figure 4a

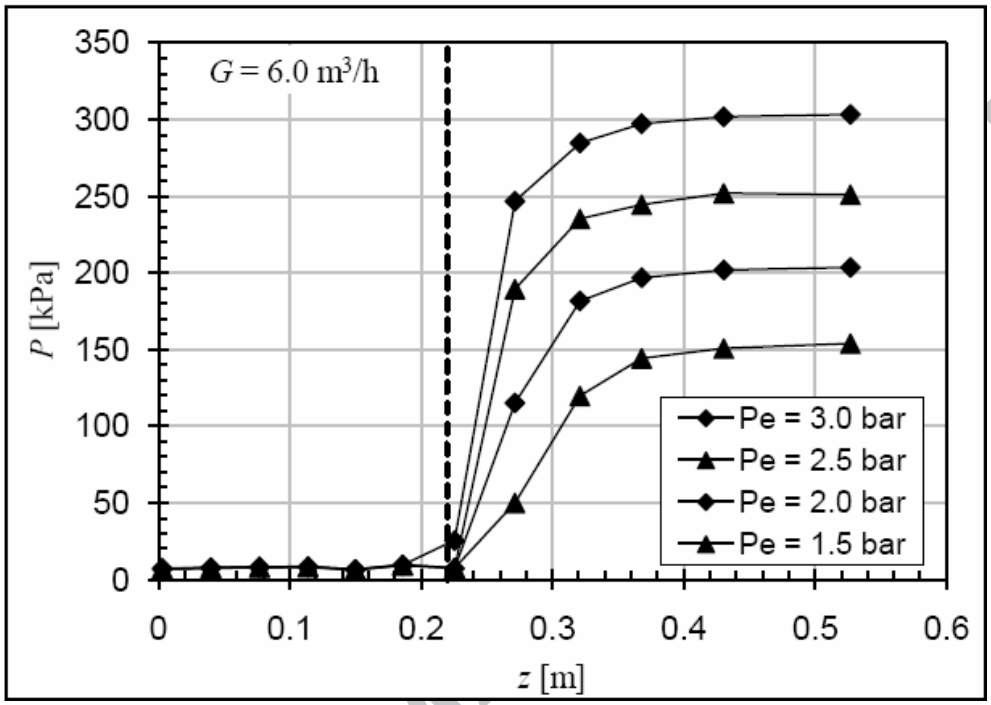

ACCEPTED MANUSCRIPT

ACCEPTED MANUSCRIPT

Figure 4b

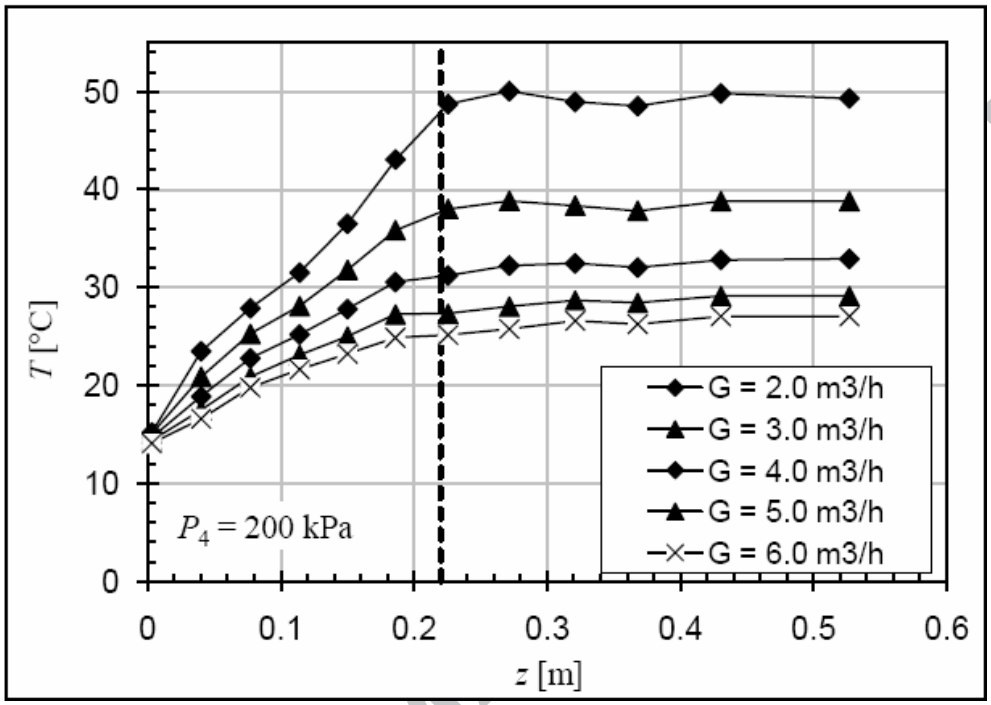

ACCEPTED MANUSCRIPT

ACCEPTED MANUSCRIPT

Figure 5a

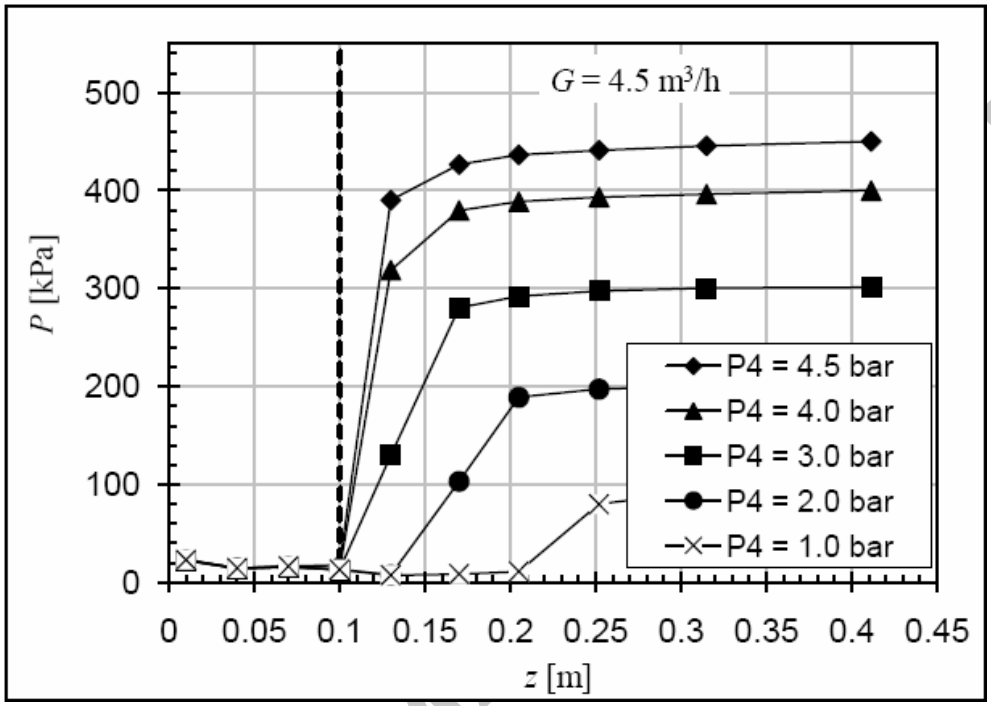

ACCEPTED MANUSCRIPT

ACCEPTED MANUSCRIPT

Figure 5b

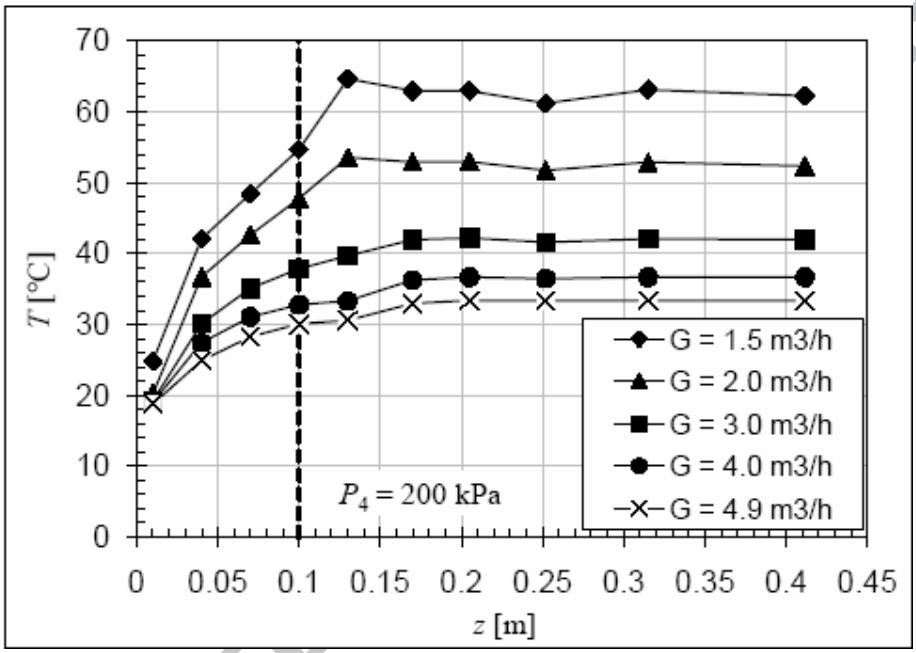

ACCEPTED MANUSCRIPT

Figure 6

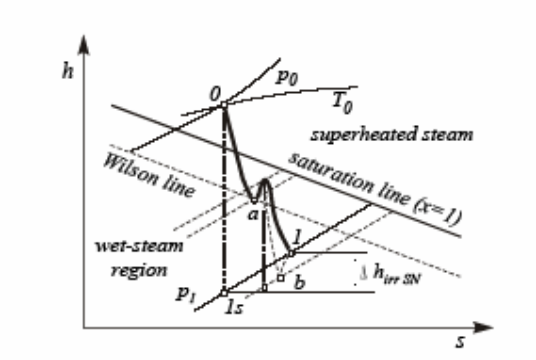

ACCEPTED MANUSCRIPT

ACCEPTED MANUSCRIPT

Figure 7

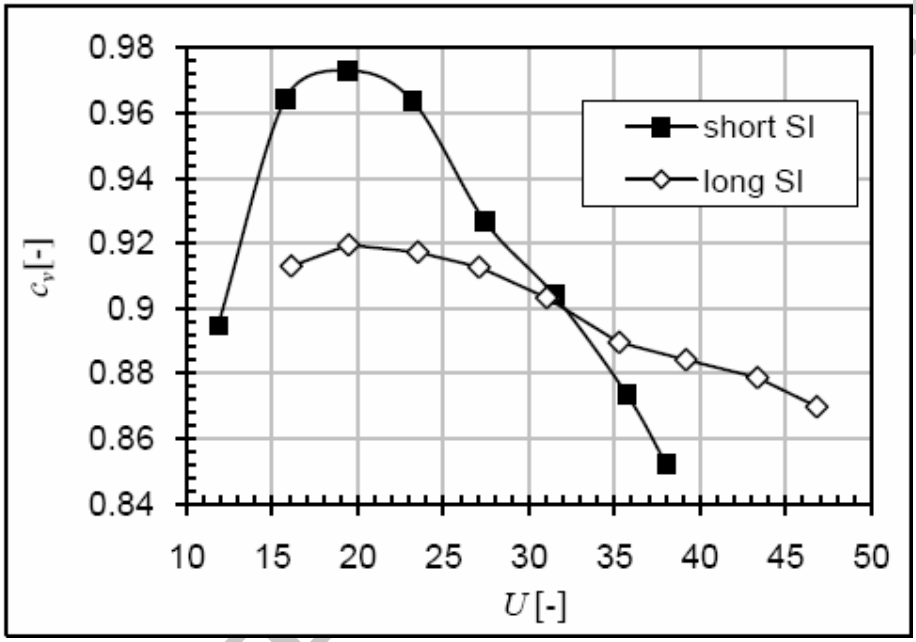

ACCEPTED MANUSCRIPT

ACCEPTED MANUSCRIPT

Figure 8a

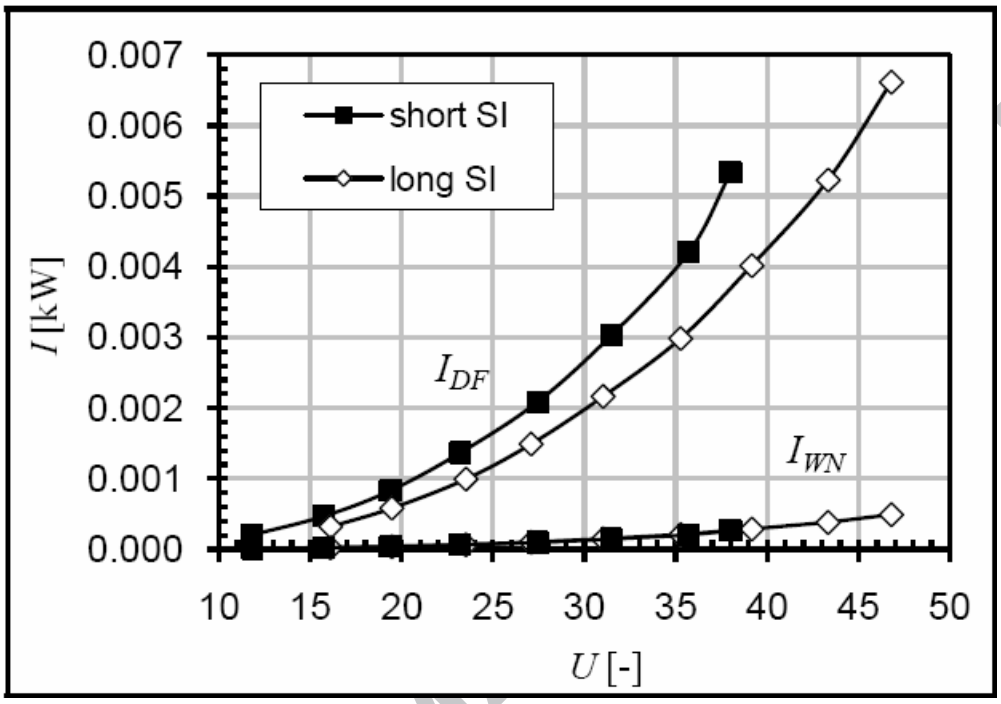

ACCEPTED MANUSCRIPT

ACCEPTED MANUSCRIPT

Figure 8b

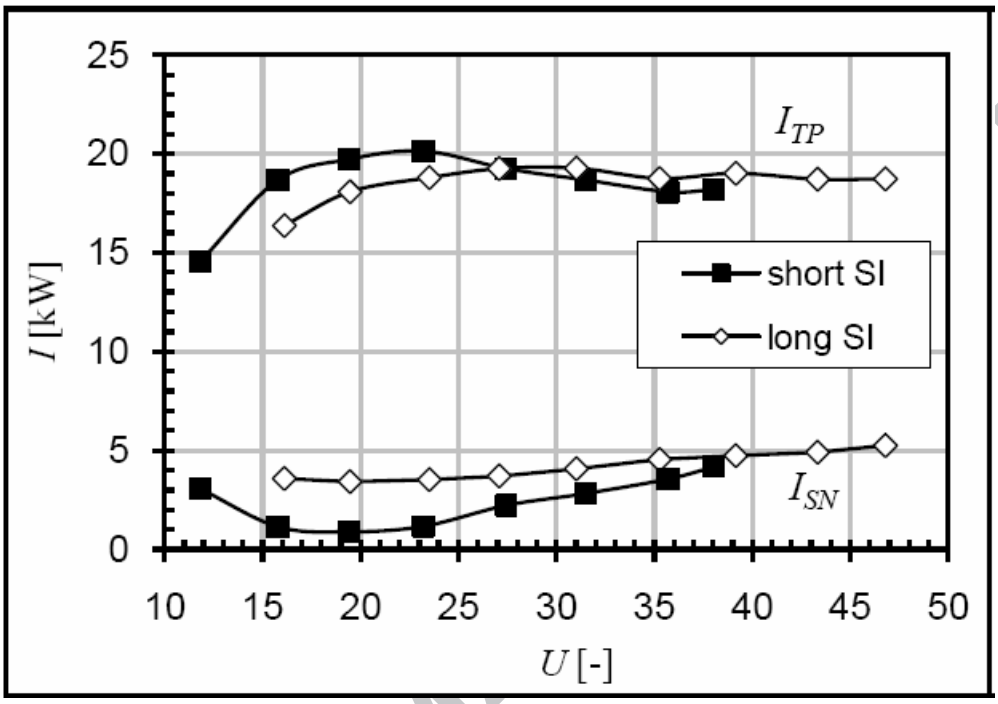

ACCEPTED MANUSCRIPT

ACCEPTED MANUSCRIPT

Figure 9

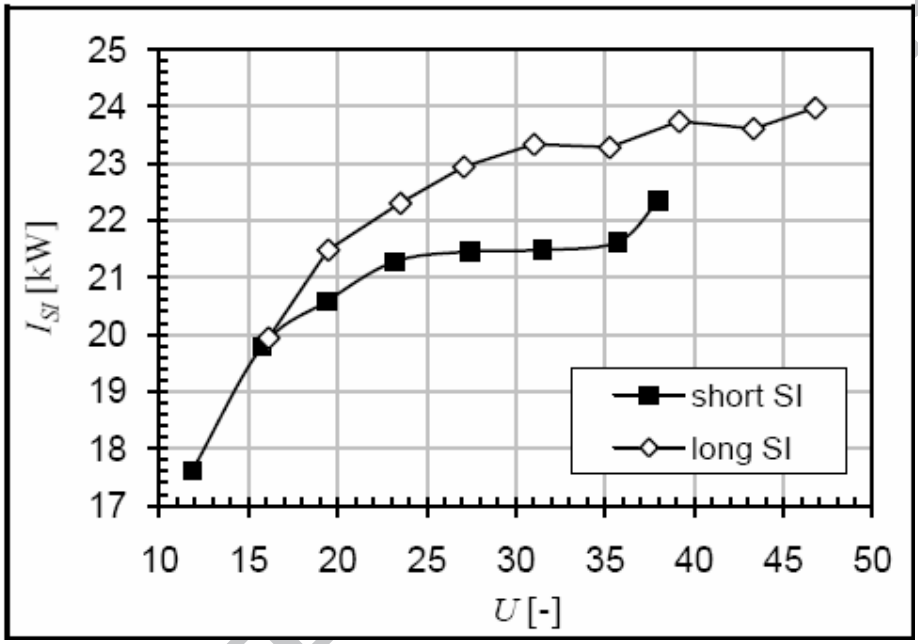

ACCEPTED MANUSCRIPT

ACCEPTED MANUSCRIPT

Figure 10a

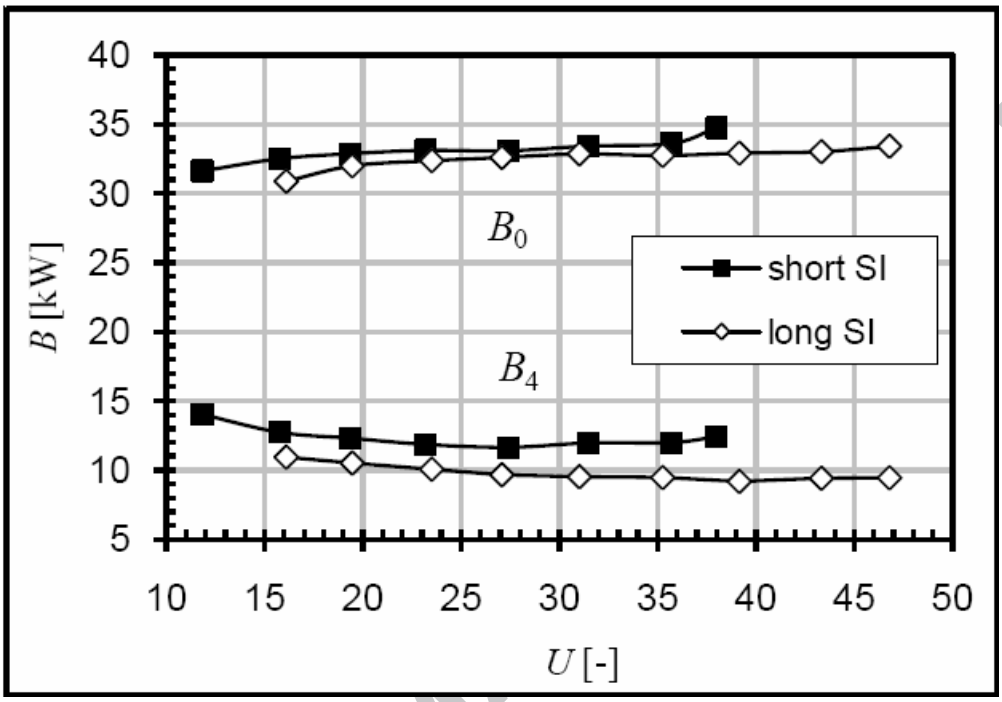

ACCEPTED MANUSCRIPT

ACCEPTED MANUSCRIPT

Figure 10b

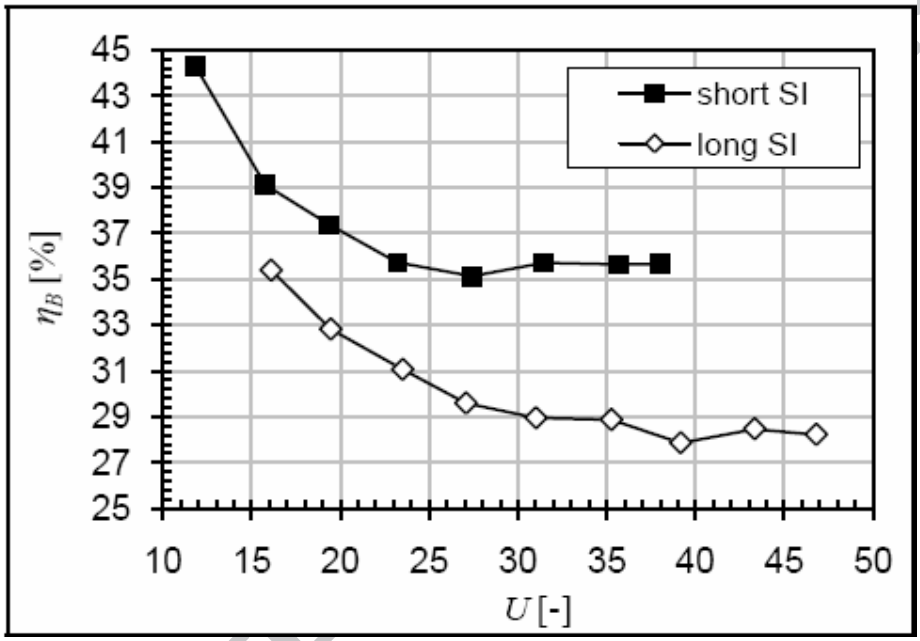

ACCEPTED MANUSCRIPT

ACCEPTED MANUSCRIPT

Fig. 1. Sketch of two-phase steam-water injector: *SN* – steam nozzle, *WN* – water nozzle,
MC – mixing chamber, *DF* – diffuser, *t* – throat.

Fig. 2. Diagram of experimental stand [4]: 1 – steam injector, 2 – water container with degasifier, 3 – steam generator, 4 – steam separator, 5 – steam superheater, 6 – pump, 7 – cooler, 8 – steam flow meter, 9 – water flow meter, 10 – steam control valve, 11 – water flow control valve, 12 – back-pressure control valve.

Fig. 3. Geometry of the test steam-water injector (short version) with pressure transducer (P) and thermocouple (T) locations.

Fig. 4. Measured profiles of pressure (a) and temperature (b) along the mixing chamber and diffuser recorded in the "long" SI for selected values of inlet water flow rate G and exit back-pressure p_4. Broken line at $z = 0.22$ m indicates the location of mixing chamber throat.

Fig. 5. Measured profiles of pressure (a) and temperature (b) along the mixing chamber and diffuser recorded in the "short" SI for selected values of inlet water flow rate G and exit back-pressure p_4. Broken line at $z = 0.1$ m indicates the location of mixing chamber throat.

Fig. 6. Schematic representation of steam expansion line in the steam nozzle: a – spontaneous condensation on Wilson line, b – shock wave at nozzle exit.

Fig. 7. Overall velocity coefficient c_v versus entrainment ratio U calculated for steam nozzles of two SI versions.

Fig. 8. Exergy losses in the injector parts calculated for the two versions of the injector.

Fig. 9. Total exergy losses calculated for two injector versions.

Fig. 10. a) Exergy rate at steam injector inlet $\dot{B}_0$ and exit $\dot{B}_4$, b) steam injector efficiency η_B versus entrainment ratio U.

ACCEPTED MANUSCRIPT